

# An actin-based cytoskeleton in archaea

Thijs J. G. Ettema,<sup>\*†</sup> Ann-Christin Lindås<sup>†</sup> and Rolf Bernander

Department of Molecular Evolution, Evolutionary Biology Center, Uppsala University, Norbyvägen 18C, SE-752 36, Uppsala, Sweden.

## Summary

**In eukaryotic and bacterial cells, spatial organization is dependent upon cytoskeletal filaments. Actin is a main eukaryotic cytoskeletal element, involved in key processes such as cell shape determination, mechanical force generation and cytokinesis. We describe an archaeal cytoskeleton which forms helical structures within *Pyrobaculum calidifontis* cells, as shown by *in situ* immunostaining. The core components include an archaeal actin homologue, Crenactin, closely related to the eukaryotic counterpart. The crenactin gene belongs to a conserved gene cluster denoted Arcade (actin-related cytoskeleton in Archaea involved in shape determination). The phylogenetic distribution of arcade genes is restricted to the crenarchaeal Thermoproteales lineage, and to Korarchaeota, and correlates with rod-shaped and filamentous cell morphologies. Whereas Arcadin-1, -3 and -4 form helical structures, suggesting cytoskeleton-associated functions, Arcadin-2 was found to be localized between segregated nucleoids in a cell subpopulation, in agreement with possible involvement in cytokinesis. The results support a crenarchaeal origin of the eukaryotic actin cytoskeleton and, as such, have implications for theories concerning the origin of the eukaryotic cell.**

## Introduction

The eukaryotic cytoskeleton is a dynamic structure comprised of protein filaments involved in the establishment and maintenance of cell shape and cellular junctions, formation of cellular protrusions (e.g. phagocytosis), and cell division. In addition, the cytoskeletal network provides a molecular scaffold that supports cellular trafficking of organelles and vesicles (Pollard and Cooper, 2009). Mature actin filaments consist of two F-actin protofila-

ments twisted around one another to form a right-handed double helix, which constitute well-characterized central components of cytoskeleton-dependent processes (Pollard and Cooper, 2009; van den Ent *et al.*, 2001). As a result of the involvement in pivotal processes, the primary structure of actin has been extremely well conserved during evolution such that, for example, actin from rabbit and yeast are 88% identical (Erickson, 2007).

Whereas the eukaryotic cytoskeleton was first described centuries ago (Frixione, 2000), the notion that bacteria also may contain cytoskeletal elements is relatively recent (Bi and Lutkenhaus, 1991; van den Ent *et al.*, 2001; Jones *et al.*, 2001). The three-dimensional structure of the bacterial cytoskeletal protein MreB was found to resemble that of actin in considerable detail (van den Ent *et al.*, 2001) and, moreover, the structure of the MreB protofilament is in remarkably good agreement with the model for F-actin, indicating close resemblance between MreB and actin assembly (van den Ent *et al.*, 2001). MreB forms large, helical, structures in rod-shaped cells (Jones *et al.*, 2001), and shape determination is thus one of the main functions of the MreB protein family (Carballido-Lopez, 2006).

Archaea constitutes the third domain of life, along with Bacteria and Eukarya (Woese *et al.*, 1990). The existence of cytoskeletal-like structures in archaea has been anticipated (Hixon and Searcy, 1993; Trent *et al.*, 1997) and rod-shaped, or filamentous, cell morphologies are abundant in several archaeal lineages, including methanogenic species, members of Thermoproteales (Zillig *et al.*, 1981) and *Candidatus* Korarchaeum cryptofilum (Elkins *et al.*, 2008). However, experimental evidence in support of cytoskeletal structures in archaea has so far not been reported, although the structural similarity to eukaryotic actin of the *Thermoplasma thermofilum* Ta0583 gene product appeared to provide evidence for such models (Roeben *et al.*, 2006; Hara *et al.*, 2007). The intracellular concentration of Ta0583 was, however, found to be too low to support an involvement in shape determination (Roeben *et al.*, 2006), and phylogenetic analyses indicate that the *Thermoplasma* protein is more closely related to proteins of the ParM family (Gerdes *et al.*, 2010), involved in chromosome partition and plasmid segregation, than to actin (Yutin *et al.*, 2009).

Certain rod-shaped methanogenic archaea contain *bona fide* MreB homologues (Jones *et al.*, 2001) and may, thus, contain a cytoskeleton based on MreB

Accepted 8 March, 2011. \*For correspondence. E-mail Thijs. Ettema@ebc.uu.se; Tel. (+46) 18 471 6129; Fax (+46) 18 471 6404. †T.J.G.E. and A.-C.L. contributed equally to this work.

protofilaments. MreB homologues have, however, not been identified in other rod-shaped archaea and cell shape-determining proteins thus remain to be identified in these species.

Here, we describe the first archaeal cytoskeleton, denoted Arcade (actin-related cytoskeleton in Archaea involved in shape determination), and identify an archaeal actin homologue, Crenactin, as a main component. Further, we describe several additional novel cytoskeletal proteins, Arcadins, unique to the archaea and which, together with Crenactin, form cell-spanning helical structures in *Pyrobaculum calidifontis*, a species belonging to the Thermoproteales order. From an evolutionary perspective, the existence of an actin-based cytoskeleton in deeply branching crenarchaeal lineages has multiple implications for models that postulate an archaeal origin of the eukaryotic cytoskeleton and, as such, for the origin of the eukaryotic cell itself.

## Results and discussion

### Identification and biochemical characterization of an archaeal actin homologue

During the course of our studies of organisms belonging to the Crenarchaeota, we focused on a *P. calidifontis* ATPase that displayed high similarity to eukaryotic actin. The archaeal homologue is encoded in all fully sequenced genomes in the crenarchaeal order Thermoproteales, as well as in *Ca. Korarchaeum cryptofilum* (Elkins *et al.*, 2008). The actin homologues belong to a large ATPase protein family that, in addition to eukaryotic actin, comprises sugar kinases, heat shock proteins, and bacterial proteins involved in cell shape determination (MreB), magnetosome organization (MamK) and plasmid segregation (ParM) (Bork *et al.*, 1992). A thorough phylogenetic analysis revealed that the crenarchaeal proteins are most closely related to eukaryotic actin (Fig. 1), suggesting a common origin, further supported by the fact that the crenarchaeal homologues exclusively share certain regions with actin to the exclusion of other members of the actin ATPase family (Yutin *et al.*, 2009). Throughout the text we refer to the crenarchaeal homologues as 'Crenactin', to differentiate the two groups while emphasizing the evolutionary link.

Recombinant Crenactin from *P. calidifontis* revealed highest activity towards ATP or GTP as nucleotide, showing only residual activity on UTP, CTP and dNTPs (Fig. 2A). In this respect, Crenactin resembles MreB which displays a similar substrate specificity (van den Ent *et al.*, 2001; Esue *et al.*, 2005), but differs from eukaryotic actin, which is active towards ATP only (Pollard and Cooper, 1986; Esue *et al.*, 2005). Crenactin ATPase activity was optimal around 0.4 mM ATP concentration

(Fig. 2B), and significantly inhibited at elevated levels. As expected, Crenactin represents the most thermoactive actin homologue studied thus far, with an optimal temperature above 90°C (Fig. 2C).

### The phylogenetic distribution of Crenactin correlates with rod-shaped and filamentous cell morphologies

Despite absence of cell shape-determining genes such as *mreB* (van den Ent *et al.*, 2001; Margolin, 2009), all Crenactin-containing species display rod-shaped or filamentous cell morphologies (Fig. 3). Typical rod-shaped *Pyrobaculum* cells measure 3–8 µm in length and 0.6 µm in diameter (Amo *et al.*, 2002), whereas *Korarchaeum* cells display an ultrathin, needle-like filamentous morphology, with cells below 0.2 µm in diameter and an average length of 15 µm, although filaments with lengths up to 100 µm also have been observed (Elkins *et al.*, 2008). As no other crenarchaeal orders appear to contain species with rod- or needle-like morphologies, the phylogenetic distribution of Crenactin matches that of filamentous cell shape within Crenarchaeota (Fig. 3). As described above certain methanogens, including *Methanothermobacter thermautotrophicus* and *Methanopyrus kandleri*, also display rod-shaped morphologies. However, these euryarchaeal species lack Crenactin-encoding genes and instead contain *bona fide* MreB orthologues (Figs 1 and 3), presumably involved in cell shape determination in these organisms. In conclusion, the phylogenetic analysis supported a model in which rod-shaped and filamentous cell morphologies in Thermoproteales and Korarchaeae are sustained by a Crenactin-based cytoskeleton.

### Crenactin forms helical structures within *P. calidifontis* cells

To confirm that Crenactin indeed is involved in shape determination, exponentially growing *P. calidifontis* cells were immunostained with antibodies raised against Crenactin. The stainings revealed cell-spanning helical structures (Fig. 4A), suggesting that Crenactin forms the backbone of an archaeal cytoskeleton. In <1% of the cells, helical filaments were absent and, instead, centrally positioned band-like structures were observed (Fig. 4B). Similar structures have been observed for MreB (Vats and Rothfield, 2007) and inferred to represent stages in cytoskeleton remodelling in preparation for cell division. Despite limited sequence similarity between Crenactin and MreB the proteins are, consequently, united by similar functional characteristics, while the phylogenetic analysis revealed that Crenactin evolutionarily is most similar to eukaryotic actins (above; see also Yutin *et al.*, 2009). Thus, as in many other molecular and cellular features, archaea appear to contain a combination of characteris-

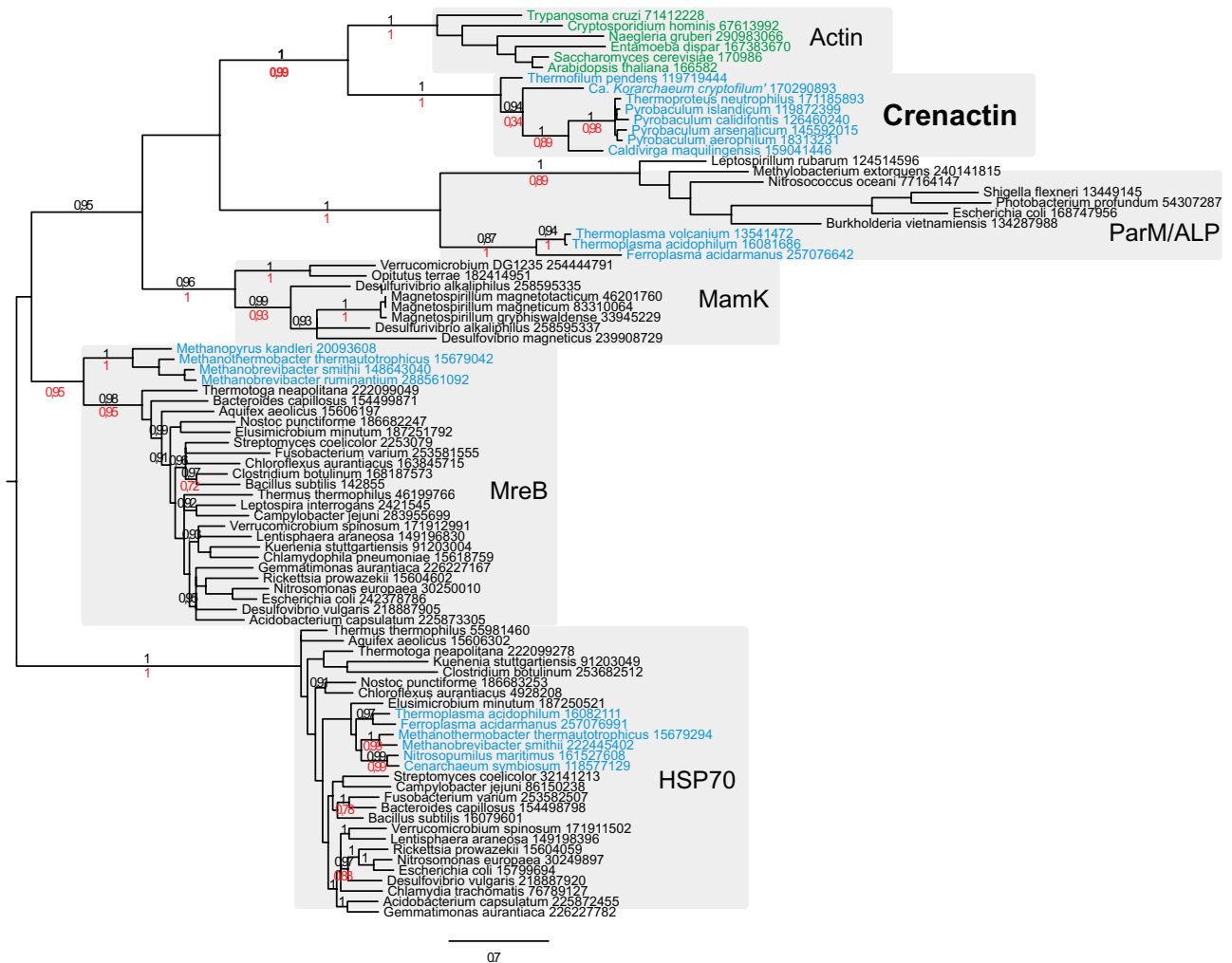


**Fig. 1.** The evolutionary history of the actin ATPase protein family. The phylogenetic tree is based on a Bayesian analysis of proteins belonging to the actin ATPase family. The actin family has recently been significantly expanded with the discovery of 35 highly divergent families of actin-like proteins (ALPs) in bacteria (Derman *et al.*, 2009), all of which form a clade that also comprises ParM-like proteins (ParM/ALP). The tree was rooted with the HSP70 protein family as outgroup and sequences are annotated by a species name followed by a gene identifier. Bayesian posterior probability (PP, black font) and parametric bootstrap support (BS, red font) values are indicated for each of the major internal branches of the tree (not within smaller monophyletic groups). PP support values below 0.90 and BS values below 0.70 were omitted from the tree and branches with PP support values below 0.50 were collapsed. Eukaryotic, archaeal and bacterial sequences are indicated in green, blue and black fonts respectively. Note that Crenactin and eukaryotic actin are inferred to share common ancestry with high support (PP = 1.00, BS = 0.99).

tics previously considered specific to either of the other two domains of life.

To investigate whether the Crenactin structures were sensitive to known cytoskeleton inhibitors, exponentially growing *P. calidifontis* cultures were exposed to varying concentrations of actin or MreB inhibitors [cytochalasin B and D (Cooper, 1987)], and S-(3,4-dichlorobenzyl)isothiourrea (A22) (Bean *et al.*, 2009) respectively. The drugs had no major effects on the growth of *P. calidifontis* cultures (not shown), nor could we find evidence that the *in vivo* integrity of the Crenactin structures was affected by drug addition (Fig. 4C). *In vitro* assays revealed that Crenactin polymerization was significantly inhibited by elevated (millimolar range) A22 con-

centrations only (Fig. 4D), thus being far less affected by this inhibitor than bacterial MreB, which is readily inhibited by micromolar concentrations (Gitai *et al.*, 2005; Bean *et al.*, 2009). These findings allude to structural or mechanistic differences in Crenactin filament dynamics, as compared with actin and MreB.

#### The Arcade (rkd) gene cluster

Comparative genome analysis is a useful tool to obtain information regarding gene function in archaeal species, which often are difficult to culture and limited in, or completely lack, genetic tractability (Ettema *et al.*, 2005), which particularly applies to members of the Thermoproteales.

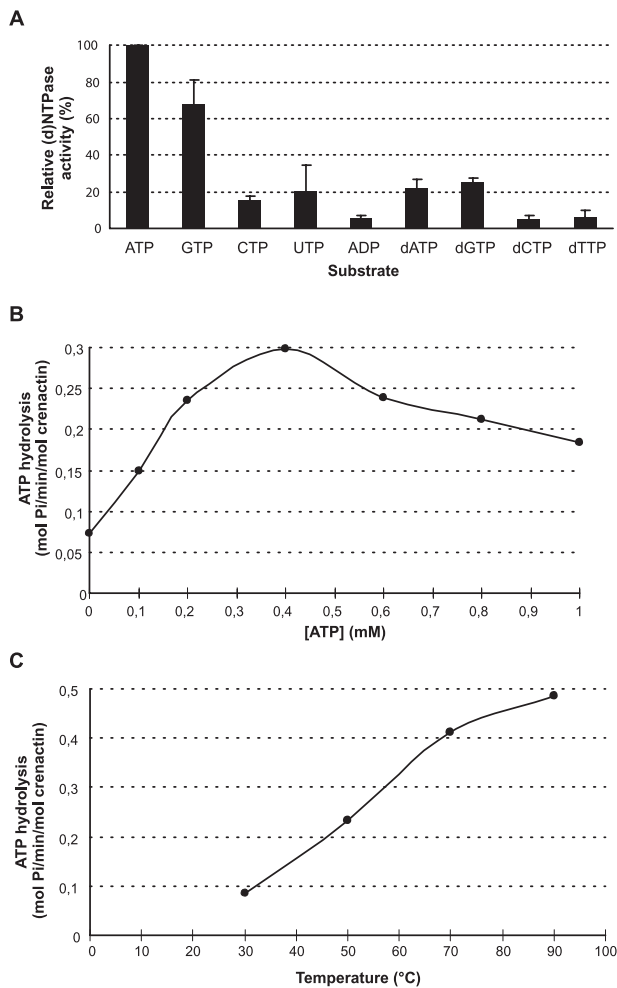


**Fig. 2.** Biochemical characterization of recombinant *P. calidifontis* Crenactin.

A. Crenactin activity at 50°C towards different nucleotides at 0.2 mM concentrations.

B. Crenactin ATPase activity as a function of ATP concentration at 50°C.

C. Crenactin ATPase activity (0.2 mM ATP concentration) at different temperatures. Due to ATP instability, temperatures above 90°C could not be tested. All assays were performed under standard conditions as described in *Experimental procedures*.

We analysed the genomes of crenactin-containing species, identifying a conserved gene cluster that, in addition to the Crenactin gene (Pcal\_1635), comprised several hypothetical genes (Fig. 5; cf. Makarova *et al.*, 2010). The clustering with the Crenactin gene, as well as the formation of distinct intracellular structures by the gene products (below), indicates a joint function in cell shape determination, and we therefore denote the gene cluster Arcade, for actin-related cytoskeleton in Archaea involved in shape determination. Except for the first gene, *rkd-1* (encoding Arcadin-1), for which a distant homologue is present in *Ca. Korarchaeum cryptofilum*, all *rkd* genes appear to be Thermoproteales-specific (Table 1). We, thus, identified

homologues of Arcadin-2 and -3 in all members of the Thermoproteales sequenced thus far (Fig. 5, Table 1) and were, consequently, unable to confirm the conclusion that these *rkd* genes are specific to the genus *Pyrobaculum* (Makarova *et al.*, 2010), nor could we corroborate the presence of *rkd-1* in members of the Thaumarchaeota reported in the same study. The Arcade gene cluster is conserved to varying degrees (Fig. 5), being identical in all *Pyrobaculum* sp. and in *Thermoproteus neutrophilus*. In *Vulcanisaeta distributa* and *Thermofilum pendens* all arcadin genes are also present, but the *rkd-1* gene is not located in the cluster. In *Caldivirga maquilingensis* the *rkd* genes are scattered across the genome, except for *rkd-3* and *rkd-4* which are adjacent.

As indicated above, most arcade gene products display no significant homology to proteins of known function. The only notable exception is Arcadin-4, which is distantly related to archaeal and bacterial SMC (structural maintenance of chromosomes) proteins and has been predicted to display ATPase activity (Makarova *et al.*, 2010). We identified a potential ATP binding site/Walker A motif at the N-terminus of Arcadin-4 proteins (Fig. 6A) supporting this prediction. In addition, we identified a domain specific to

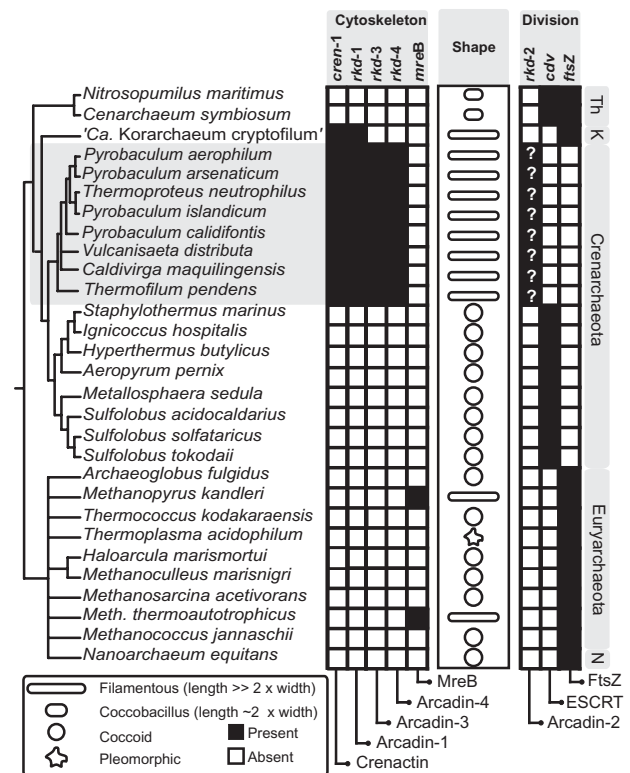


**Fig. 3.** Phylogenetic distribution of cell shape-determining and cell division proteins in archaeal genomes. Rod-shaped or filamentous cell morphologies in archaeal species correlate with the presence of Crenactin/Arcadin-1 or MreB. Species belonging to the order Thermoproteales are shaded in grey. Abbreviations: Th, Thaumarchaeota; K, Korarchaeota; N, Nanoarchaeota.

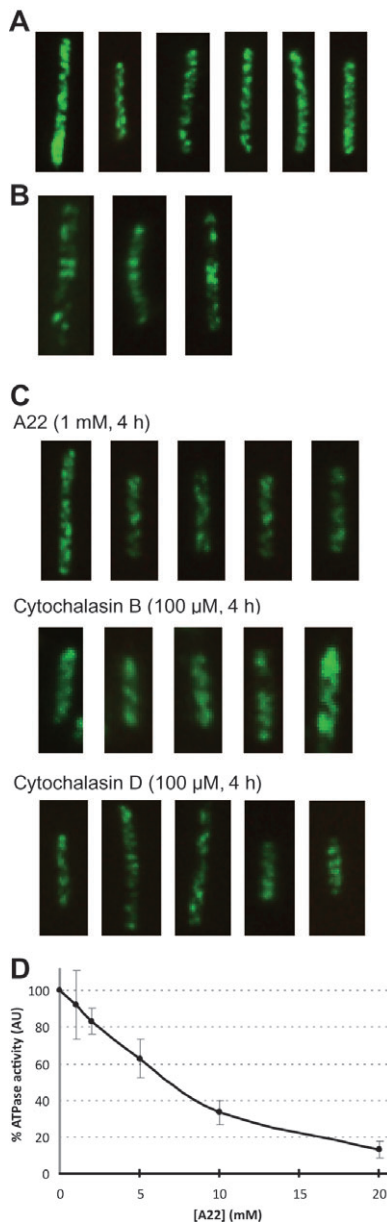


**Fig. 4.** *In situ* immunofluorescence microscopy of exponentially growing *P. calidifontis* cells stained with anti-Crenactin antibodies. **A.** Cell-spanning helical filaments. **B.** Examples of subpopulation of cells displaying centrally located band-like structures. **C.** Immunostainings of cells incubated with A22 (upper panel) or the actin inhibitors Cytochalasin B and D (middle and lower panel respectively) for 4 h at the indicated concentrations. **D.** *In vitro* inhibition of crenactin polymerization by A22.

Smc proteins (Fig. 6B) and several predicted coiled-coil regions (Fig. 6B and C). Altogether these findings support the idea that Arcadin-4 might play an Smc-like role in chromosome condensation and, given the apparent association with cytoskeletal proteins, could be involved in the process of genome segregation. The *rkd-2* gene is positioned directly adjacent to the Crenactin-encoding gene

(*cren-1*), and the gene product contains several predicted coiled-coil motifs. Although coiled-coils are common in a variety of protein families it is noteworthy that, in eukaryotes, several proteins that either interact with actin directly, or are involved in remodelling of actin networks (plectin, myosin, tropomyosin), also contain coiled-coils. The *rkd-3* gene encodes a small polypeptide of about 6.5 kDa in size, which, again, lacks homology to any protein outside the Thermoproteales.

#### *Arcadin* proteins form helical structures that span *P. calidifontis* cells

Next, we investigated whether the genes that comprise the gene cluster have potential cytoskeletal functions, in addition to Crenactin. Antibodies were raised against all proteins encoded by the *P. calidifontis* arcade genes, and *in situ* immunostainings revealed that Arcadin-1, -3 and -4 formed helix-like structures that closely resembled those formed by Crenactin (Fig. 7A–C). In contrast, the staining patterns observed with Arcadin-2 (below) differed markedly from those formed by Crenactin and the other Arcadins. The helical structures formed by Arcadin-1 colocalized with those formed by Crenactin, as evidenced by *P. calidifontis* cells double-stained with the respective antibodies (Fig. 7D). Based on these observations, we speculate that Arcadin-1 and Crenactin physically interact and form part of the same helical protein complex. Still, close observation of the double stainings revealed minor differences in intensity, and the patterns did not always fully overlap (Fig. 7D). It remains to be determined whether these differences are biologically significant, or whether they result from technical variation e.g. in staining efficiency or the precise focal plane in the microscopy.

The helical structures formed by Arcadin-3 and -4 were occasionally less pronounced, and in some cases punctuated in appearance (Fig. 7B and C respectively). This could indicate that Arcadin-3 and -4 interacted with a helical backbone formed by Crenactin and Arcadin-1, rather than being primary components in shaping this structure. Irrespective, all gene products of the cluster appeared to form part of an Arcade-based cytoskeleton.

We did not observe band-like structures, such as those observed for Crenactin (Fig. 4B), for any of the Arcadin proteins, indicating that the reorganization of the helical structures in preparation for cytokinesis occurred along different routes for different cytoskeletal components.

#### *Localization of Arcadin-2 between segregating nucleoids*

Immunostainings of exponentially growing *P. calidifontis* cell populations with antibodies against Arcadin-2

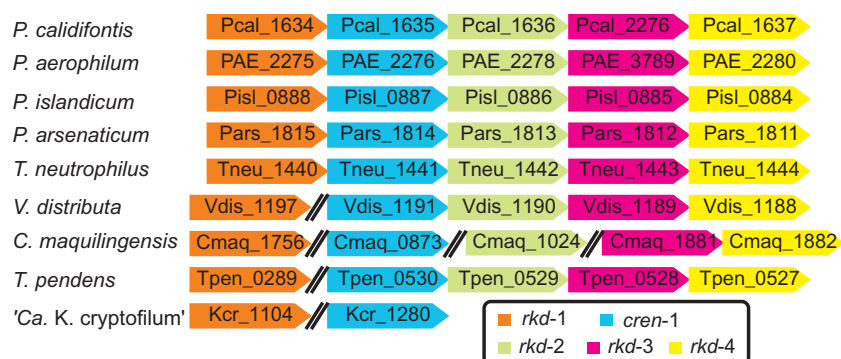


**Fig. 5.** Conservation of the arcade gene cluster across crenarchaeal genomes. The genes comprising the arcade cluster are depicted as follows: crenactin (blue), *rkd-1* (orange), *rkd-2* (green), *rkd-3* (magenta) and *rkd-4* (yellow).

revealed punctuated patterns, generally consisting of up to three distinct fluorescence foci per cell (Fig. 8A). In a subpopulation, a single focus was observed in the centre of the cells. Intrigued by this observation, which suggested that Arcadin-2 might fulfil a role in cytokinesis, we performed stainings with a combination of antibodies and 4',6-diamidino-2-phenylindole (DAPI). Such double stainings of *P. calidifontis* cells turned out to be technically challenging, but in stainings in which acceptable resolution was obtained, most cells in which Arcadin-2 was centrally positioned contained segregated nucleoids that flanked the antibody focus (Fig. 8B). Occasionally, short cells were observed that contained a single fluorescence focus at the extreme end (Fig. 8C). Assuming that these cells recently had undergone division, the polar localization of Arcadin-2 indicates that the protein remained at one of the newly formed poles after cell scission. Together, the observations point to a role for Arcadin-2 in the cytokinesis process, although further studies will be necessary to substantiate a cell division function.

We have previously noted that genes encoding *ftsZ*- or *cdv*-based cell division systems are absent in Thermoproteales genomes (Lindås *et al.*, 2008; Ettema and Bernander, 2009) (Fig. 3, right panel), in line with the possibility that a specific constriction machinery may not exist in these organisms (Sonobe *et al.*, 2010; Bernander and Ettema, 2010). Still, possible cytokinesis-related functions would be expected to reside within a Thermoproteales-specific gene set and, interestingly, the

Arcadin-2 gene belongs to a subset of 15 genes specific to all Thermoproteales, which also includes *rkd-3* and -4 (Table 2). This would, thus, agree with a possible division-associated function for Arcadin-2, whereas Arcadin-3 and -4 primarily would appear to be involved in shape determination. The gene organization would ensure a tight connection between cytoskeletal reorganization and cell division and it is, thus, possible that these functions are united in the Arcade complex through formation of a core cytoskeleton by Crenactin and Arcadin-1, with Arcadin-3 and -4 performing auxiliary roles and Arcadin-2 providing a link to the cytokinesis process. The Smc-like nature of Arcadin-4 (Fig. 6) makes this protein a good candidate for involvement in the process of genome condensation and/or segregation (above).

#### Implications for eukaryogenesis

From an evolutionary perspective, the existence of actin-based cytoskeletal structures in Archaea bears relevance for the origin of the eukaryotic cytoskeleton and, perhaps, even the eukaryotic lineage itself. Although the deep roots of archaeal phylogeny are currently under debate (Gribaldo *et al.*, 2010), recent phylogenetic studies that accommodate across-site as well as across-tree compositional heterogeneity have provided evidence in support of the 'eocyte' hypothesis (Cox *et al.*, 2008). This suggests that extant eukaryotes evolved from a proto-eukaryotic lineage that shares common ancestry with

**Table 1.** The arcade (*rkd*) gene cluster.

| Gene name     | Protein name | Size <sup>a</sup> | Phylogenetic distribution    | Homology   |
|---------------|--------------|-------------------|------------------------------|--|
| <i>rkd-1</i>  | Arcadin-1    | 12.4 (Pcal_1634)  | Thermoproteales, Korarchaeum | –  |
| <i>cren-1</i> | Crenactin    | 48.4 (Pcal_1635)  | Thermoproteales, Korarchaeum | Actin (distantly related to MamK, ParM, MreB and Hsp70)                        |
| <i>rkd-2</i>  | Arcadin-2    | 22.6 (Pcal_1636)  | Thermoproteales              | –  |
| <i>rkd-3</i>  | Arcadin-3    | 6.4 (Pcal_2276)   | Thermoproteales              | –  |
| <i>rkd-4</i>  | Arcadin-4    | 90.2 (Pcal_1637)  | Thermoproteales              | SMC-like, distant homologs present in some Archaea and bacterial thermophiles. |

a. Size in kDa based on the calculated weight of the respective *P. calidifontis* proteins, as indicated between brackets.

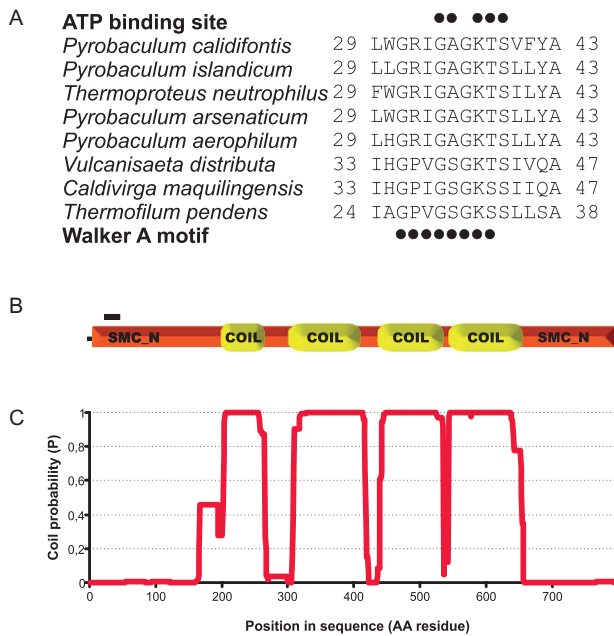


**Fig. 6.** Arcadin-4 is an Smc-like protein.

A. Protein sequence analysis of Arcadin-4 orthologues present in Thermoproteales. The ATP binding site and Walker A motif are indicated by filled circles above and below the subalignment respectively.

B. Similarity across the entire Arcadin-4 protein sequence to an SMC\_N-type domain (Finn *et al.*, 2010). The black bar indicates the position of the ATP binding site and Walker A motif.

C. Predicted coiled-coil regions (Lupas *et al.*, 1991) throughout the Arcadin-4 protein sequence.

Crenarchaeota (Lake *et al.*, 1984; Baldauf *et al.*, 1996; Hashimoto and Hasegawa, 1996), or with a presumed common ancestor of the Crenarchaeota and Thaumarchaeota lineages (Foster *et al.*, 2009). Although the current complement of sequenced archaeal genomes appears significantly under-sampled compared with the archaeal diversity observed in environmental surveys (e.g. Nunoura *et al.*, 2010), these studies point towards a scenario in which Eukarya evolved from a lineage within the Archaea, rather than as a sister clade. Irrespective, in most contemporary models that address the origin of the eukaryotic cell, a cytoskeleton is regarded a *sine qua non*, as it would have facilitated phagocytosis of participating organisms (e.g. Cavalier-Smith, 2002; Poole and Penny, 2007; Yutin *et al.*, 2009). Hence, the existence of an actin-based cytoskeleton in deep crenarchaeal lineages adds an important piece to the evolutionary puzzle, as it could have provided primitive phagocytotic capabilities to the proto-eukaryote (Yutin *et al.*, 2009), such as the ability to form membrane protrusions. Eventually, this primordial actin-based machinery could, in initial stages of eukaryogenesis, have facilitated the engulfment of the proto-mitochondrion, thereby jump-starting the evolution of the eukaryotic cell.

## Experimental procedures

### Strains, growth conditions and in vivo inhibition experiments

*P. caldifontis* cells were cultivated in TY medium supplemented with 0.3% sodium thiosulphate using shaking water-baths at 90°C as described previously (Amo *et al.*, 2002). For experiments designed to test sensitivity towards cytoskeleton inhibitors, exponentially growing *P. caldifontis* cultures were exposed to varying concentrations of Cytochalasin B and D and A22 for 4 h. Aliquots were taken at defined time intervals to measure cell density (at OD<sub>660</sub>) and to inspect cell morphology and formation of cytoskeletal elements using microscopy as described below.

### PCR amplification, cloning and transformation

*P. caldifontis* genomic DNA was extracted as described previously (Lundgren *et al.*, 2004). Target genes Pcal\_1634, Pcal\_1635, Pcal\_1636, Pcal\_2276 and Pcal\_1637 were PCR-amplified using oligonucleotide combinations 5'-atagatccatggccactattaggggcatc-3' and 5'-atagatccttaagcttctggctttacctaat-3' (Pcal\_1634), 5'-atagatcccatggcgctgattcagagcgc-3' and 5'-atagatcctcagcggcgctggaacct-3' (Pcal\_1635),

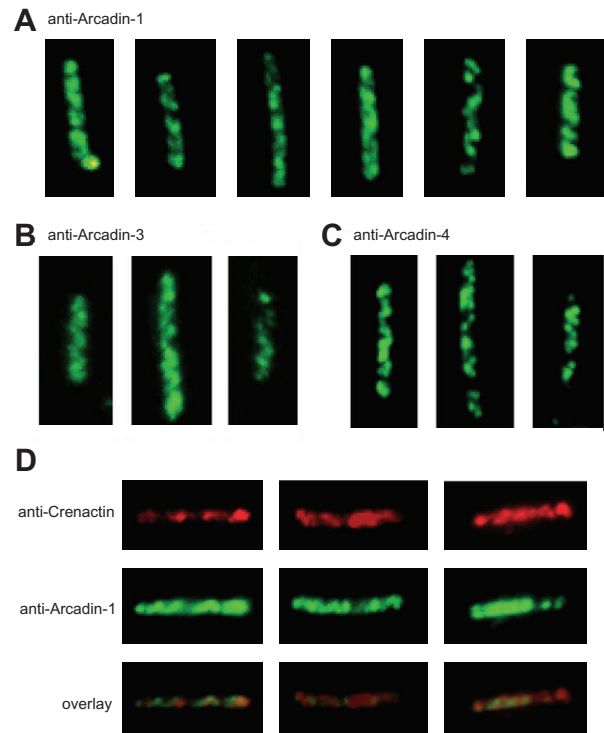


**Fig. 7.** *In situ* immunostainings with anti-Arcadin-1, -3 and -4 antibodies.

A–C. *In situ* immunofluorescence microscopy of exponentially growing *P. caldifontis* cells stained with (A) anti-Arcadin-1, (B) anti-Arcadin-3 and (C) anti-Arcadin-4 antibodies.

D. Double staining with anti-Arcadin-1 (green) and Crenactin antibodies (red).

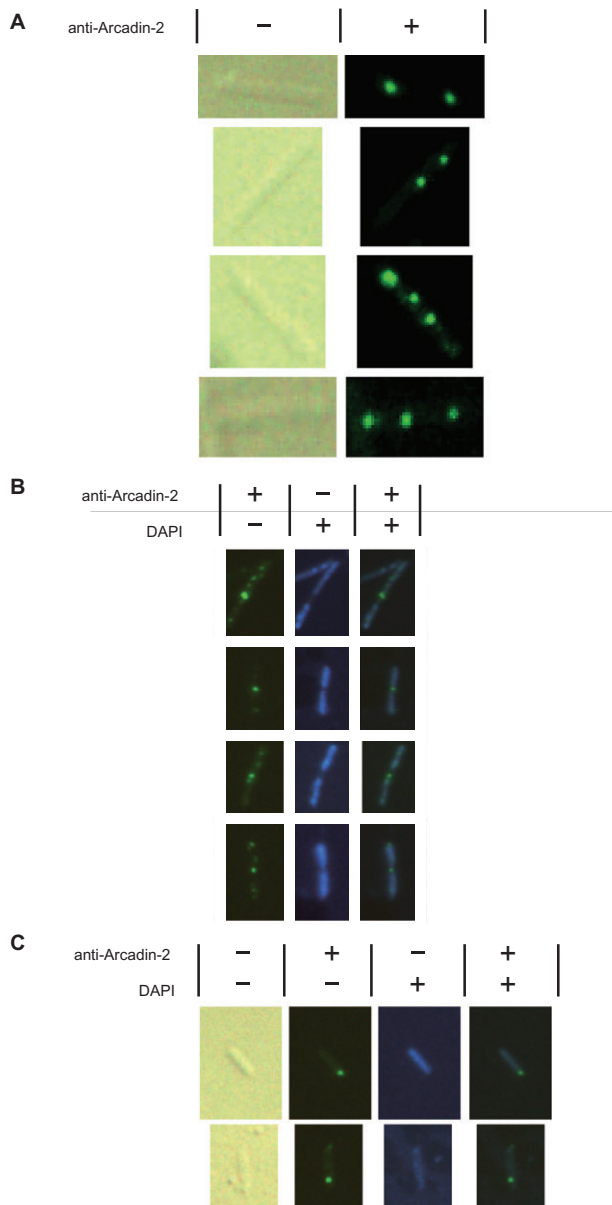


**Fig. 8.** *In situ* immunostainings with anti-Arcadin-2 antibodies. A. *In situ* immunofluorescence microscopy of exponentially growing *P. calidifontis* cells stained with anti-Arcadin-2 antibodies (green). B. Double staining with anti-Arcadin-2 antibodies (green) and the DNA-specific DAPI dye (blue). C. Short cells displaying a single fluorescence focus at the extreme end.

5'-ataggatcccctggattttccaaggtctc-3' and 5'-ataggatccctagcgcttcgacctaatgat-3' (Pcal\_1636), 5'-ataggatccctggacatctctctgagga-3' and 5'-ataggatcctcaactctcgatccgccac-3' (Pcal\_2276), and 5'-ataggatcccctgtggcggatccgagagt-3' and 5'-ataggatcctcagctttgtaaccctctatc-3' (Pcal\_1637) according to standard conditions. The obtained PCR products were cloned using *Bam*HI into the pET-45b(+) expression vector (Novagen), which adds an N-terminal 6xHis-tag to the expressed protein. Inserted sequences were verified by DNA sequencing (Big Dye Terminator v3.1 Cycle Sequencing kit,

Applied Biosystems) prior to transformation of *Escherichia coli* Rosetta (DE3) cells by electroporation.

#### *Protein expression and purification, and antibody generation*

Recombinant, histidine-tagged protein was overexpressed in *E. coli* Rosetta (DE3) and purified using the His GraviTrap system (GE Healthcare) as described in Lindås *et al.* (2008). Prior to antibody production, imidazole was removed from the respective protein fraction using a PD-10 column (GE Healthcare) according to the manufacturers' instructions. Antibodies against purified proteins were generated by Innovagen (Lund, Sweden). Antibodies against Pcal\_1634, Pcal\_1636 and Pcal\_1637 were raised in chicken and antibodies against Pcal\_1635 and Pcal\_2276 were raised in rabbit.

#### *In vitro Crenactin ATPase assays*

Crenactin polymerization was indirectly measured by assaying phosphate release using the High sensitivity ATPase assay kit (Innova Biosciences) according to the manufacturer's instructions. Standard polymerization reactions contained 50 mM Tris-HCl (pH 7.5), 200  $\mu$ M nucleotide, 2.5 mM MgCl<sub>2</sub>, 50 mM imidazole and Crenactin (6  $\mu$ M) and were incubated at 50°C for 20 min. Reactions were terminated by addition of 'PiColorLock Gold' reagent (Innova Biosciences) and allowed further incubation at room temperature followed by determination of absorbance at 635 nm using a ND-1000 Spectrophotometer (NanoDrop). Crenactin inhibition by known MreB and actin inhibitors was determined by adding varying concentrations of inhibitors dissolved in dimethyl sulphoxide (DMSO) to the standard polymerization assays.

#### *Immunostaining and microscopy*

Samples from *P. calidifontis* cell cultures were diluted in ice-cold ethanol to a final ethanol concentration of 70%. Cells were immunostained with primary antibodies against the respective target protein and secondary antibodies (Alexa Fluor 488 goat anti-chicken IgG and goat anti-rabbit IgG and Alexa Fluor 568 goat anti-chicken IgG and goat anti-rabbit IgG) for visualization by fluorescence microscopy as described in Lindås *et al.* (2008). The immunostained cells were placed on a glass slide with a layer of 1% agarose containing 1.0  $\mu$ g ml<sup>-1</sup> DAPI and visualized at 1000-fold magnification with a DMRXE epifluorescence microscope (Leica) as described previously (Lindås *et al.*, 2008).

#### *Phylogenetic analysis of actin homologues*

An alignment of actin homologues was constructed using MAFFT (Kato *et al.*, 2009) followed by manual improvement wherever necessary. Next, a Bayesian phylogenetic analysis was performed using Phylobayes (version 3.2f) with the CAT model, which accommodates across-site compositional heterogeneity (Lartillot and Philippe, 2004). Two independent chains were run for 250 000 cycles, with sampling every 50 cycles. The maximum discrepancy of bipartition frequencies

**Table 2.** Archaeal orthologous groups specific to Thermoproteales.

| arCOG <sup>a</sup> | <i>P. calidifontis</i> gene | Annotation <sup>a</sup>                                      |
|--------------------|-----------------------------|--|
| arCOG00431         | Pcal_0999                   | Predicted phosphohydrolase (DHH superfamily)                 |
| arCOG00599         | Pcal_1247                   | ATPase involved in chromosome partitioning, ParA family      |
| arCOG00741         | Pcal_1081                   | Transcriptional regulator containing HTH domain, ArsR family |
| arCOG01882         | Pcal_2060                   | Dolichol kinase  |
| arCOG03733         | Pcal_0044                   | Uncharacterized conserved protein                            |
| arCOG03746         | Pcal_0656                   | Uncharacterized conserved protein                            |
| arCOG03760         | Pcal_1080                   | Uncharacterized conserved protein                            |
| arCOG05487         | Pcal_0703                   | Uncharacterized conserved protein                            |
| arCOG05515         | Pcal_0874                   | Uncharacterized conserved protein                            |
| arCOG05523         | Pcal_0602                   | Uncharacterized conserved protein                            |
| arCOG05582         | Pcal_1634                   | Arcadin-1  |
| arCOG05583         | Pcal_1635                   | Crenactin  |
| arCOG05585         | Pcal_1637                   | Arcadin-4  |
| arCOG05654         | Pcal_1094                   | Uncharacterized conserved protein                            |
| arCOG05666         | Pcal_1792                   | Calcineurin-like phosphoesterase                             |

a. Orthology assignments and annotations (except for genes characterized in the current study) were extracted from the archaeal clusters of orthologous groups (ArCOGs) (Makarova *et al.*, 2007). Note that, due to the fact that the genome of '*Ca. Korarchaeum cryptofilum*' was not included in the ArCOG database, Arcadin-1 is listed here as 'Thermoproteales specific'. In addition, despite that Arcadin-2 and -3 (arCOG05584 and arCOG07432, respectively) are truly specific to the Thermoproteales, these proteins were not retrieved in the ArCOG screen. This was due to the fact that Arcadin-3 orthologs were initially missed in the annotation of the genomes of *Pyrobaculum aerophilum* and *P. calidifontis*, and because the Arcadin-2 ortholog of *T. pendens* shows only distant sequence similarity to the other Arcadin-2 proteins.

[as judged by bpcomp (Lartillot and Philippe, 2004)] between runs was below 0.05. The first 25 000 cycles from each run were discarded as burn-in, and a majority-rule consensus tree with branch posterior probabilities was generated from the remaining trees. The same alignment was used to perform a maximum likelihood analysis using RAxML (version 7.2.8) (Stamatakis and Ott, 2008), using the LG+G+I model of protein evolution, which was selected using ProtTest (version 2.4) (Abascal *et al.*, 2005). Support values were derived from 100 bootstrap replicates.

## Acknowledgements

This work was supported by Grants 621-2010-5551 and 621-2009-4813 from the Swedish Research Council to R.B. and T.J.G.E., respectively, a Strong Research Environment grant (Uppsala Microbiomics Center) from the Swedish Research Council for Environment, Agricultural Sciences and Spatial Planning to R.B., and by Marie Curie IEF and ERG grants (European Union) to T.J.G.E.

## References

Abascal, F., Zardoya, R., and Posada, D. (2005) ProtTest: selection of best-fit models of protein evolution. *Bioinformatics* **21**: 2104–2105.

Amo, T., Paje, M.L., Inagaki, A., Ezaki, S., Atomi, H., and Imanaka, T. (2002) *Pyrobaculum calidifontis* sp. nov., a novel hyperthermophilic archaeon that grows in atmospheric air. *Archaea* **1**: 113–121.

Baldauf, S.L., Palmer, J.D., and Doolittle, W.F. (1996) The root of the universal tree and the origin of eukaryotes based on elongation factor phylogeny. *Proc Natl Acad Sci USA* **93**: 7749–7754.

Bean, G.J., Flickinger, S.T., Westler, W.M., McCully, M.E., Sept, D., Weibel, D.B., and Amann, K.J. (2009) A22 disrupts the bacterial actin cytoskeleton by directly binding

and inducing a low-affinity state in MreB. *Biochemistry* **48**: 4852–4857.

Bernander, R., and Ettema, T.J. (2010) FtsZ-less cell division in archaea and bacteria. *Curr Opin Microbiol* **6**: 747–752.

Bi, E., and Lutkenhaus, J. (1991) FtsZ ring structure associated with division in *Escherichia coli*. *Nature* **354**: 161–164.

Bork, P., Sander, C., and Valencia, A. (1992) An ATPase domain common to prokaryotic cell cycle proteins, sugar kinases, actin, and hsp70 heat shock proteins. *Proc Natl Acad Sci USA* **89**: 7290–7294.

Carballido-Lopez, R. (2006) The bacterial actin-like cytoskeleton. *Microbiol Mol Biol Rev* **70**: 888–909.

Cavalier-Smith, T. (2002) The phagotrophic origin of eukaryotes and phylogenetic classification of Protozoa. *Int J Syst Evol Microbiol* **52**: 297–354.

Cooper, J.A. (1987) Effects of cytochalasin and phalloidin on actin. *J Cell Biol* **105**: 1473–1478.

Cox, C.J., Foster, P.G., Hirt, R.P., Harris, S.R., and Embley, T.M. (2008) The archaeobacterial origin of eukaryotes. *Proc Natl Acad Sci USA* **105**: 20356–20361.

Derman, A.I., Becker, E.C., Truong, B.D., Fujioka, A., Tucey, T.M., Erb, M.L., *et al.* (2009) Phylogenetic analysis identifies many uncharacterized actin-like proteins (Alps) in bacteria: regulated polymerization, dynamic instability and treadmilling in Alp7A. *Mol Microbiol* **73**: 534–552.

Elkins, J.G., Podar, M., Graham, D.E., Makarova, K.S., Wolf, Y., Randau, L., *et al.* (2008) A korarchaeal genome reveals insights into the evolution of the Archaea. *Proc Natl Acad Sci USA* **105**: 8102–8107.

van den Ent, F., Amos, L.A., and Löwe, J. (2001) Prokaryotic origin of the actin cytoskeleton. *Nature* **413**: 39–44.

Erickson, H.P. (2007) Evolution of the cytoskeleton. *Bioessays* **29**: 668–677.

Esue, O., Cordero, M., Wirtz, D., and Tseng, Y. (2005) The assembly of MreB, a prokaryotic homolog of actin. *J Biol Chem* **280**: 2628–2635.

Ettema, T.J., and Bernander, R. (2009) Cell division and the

- ESCRT complex: a surprise from the archaea. *Commun Integr Biol* **2**: 86–88.
- Ettema, T.J., de Vos, W.M., and van der Oost, J. (2005) Discovering novel biology by in silico archaeology. *Nat Rev Microbiol* **3**: 859–869.
- Finn, R.D., Mistry, J., Tate, J., Coggill, P., Heger, A., Pollington, J.E., *et al.* (2010) The Pfam protein families database. *Nucleic Acids Res* **38**: D211–D222.
- Foster, P.G., Cox, C.J., and Embley, T.M. (2009) The primary divisions of life: a phylogenomic approach employing composition-heterogeneous methods. *Philos Trans R Soc Lond B Biol Sci* **364**: 2197–2207.
- Frixione, E. (2000) Recurring views on the structure and function of the cytoskeleton: a 300-year epic. *Cell Motil Cytoskeleton* **46**: 73–94.
- Gerdes, K., Howard, M., and Szardenings, F. (2010) Pushing and pulling in prokaryotic DNA segregation. *Cell* **141**: 927–942.
- Gitai, Z., Dye, N.A., Reisenauer, A., Wachi, M., and Shapiro, L. (2005) MreB actin-mediated segregation of a specific region of a bacterial chromosome. *Cell* **120**: 329–341.
- Gribaldo, S., Poole, A.M., Daubin, V., Forterre, P., and Brochier-Armanet, C. (2010) The origin of eukaryotes and their relationship with the Archaea: are we at a phylogenomic impasse? *Nat Rev Microbiol* **8**: 743–752.
- Hara, F., Yamashiro, K., Nemoto, N., Ohta, Y., Yokobori, S.-I., Yasunaga, T., *et al.* (2007) An actin homolog of the archaeon *Thermoplasma acidophilum* that retains the ancient characteristics of eukaryotic actin. *J Bacteriol* **189**: 2039–2045.
- Hashimoto, T., and Hasegawa, M. (1996) Origin and early evolution of eukaryotes inferred from the amino acid sequences of translation elongation factors 1alpha/Tu and 2/G. *Adv Biophys* **32**: 73–120.
- Hixon, W.G., and Searcy, D.G. (1993) Cytoskeleton in the archaeobacterium *Thermoplasma acidophilum*? Viscosity increase in soluble extracts. *Biosystems* **29**: 151–160.
- Jones, L.J., Carballido-Lopez, R., and Errington, J. (2001) Control of cell shape in bacteria: helical, actin-like filaments in *Bacillus subtilis*. *Cell* **104**: 913–922.
- Katoh, K., Asimenos, G., and Toh, H. (2009) Multiple alignment of DNA sequences with MAFFT. *Methods Mol Biol* **537**: 39–64.
- Lake, J.A., Henderson, E., Oakes, M., and Clark, M.W. (1984) Eocytes: a new ribosome structure indicates a kingdom with a close relationship to eukaryotes. *Proc Natl Acad Sci USA* **81**: 3786–3790.
- Lartillot, N., and Philippe, H. (2004) A Bayesian mixture model for across-site heterogeneities in the amino-acid replacement process. *Mol Biol Evol* **21**: 1095–1109.
- Lindås, A.-C., Karlsson, E.A., Lindgren, M.T., Ettema, T.J., and Bernander, R. (2008) A unique cell division machinery in the Archaea. *Proc Natl Acad Sci USA* **105**: 18942–18946.
- Lundgren, M., Andersson, A., Chen, L., Nilsson, P., and Bernander, R. (2004) Three replication origins in *Sulfolobus* species: synchronous initiation of chromosome replication and asynchronous termination. *Proc Natl Acad Sci USA* **101**: 7046–7051.
- Lupas, A., Van Dyke, M., and Stock, J. (1991) Predicting coiled coils from protein sequences. *Science* **252**: 1162–1164.
- Makarova, K.S., Sorokin, A.V., Novichkov, P.S., Wolf, Y.I., and Koonin, E.V. (2007) Clusters of orthologous genes for 41 archaeal genomes and implications for evolutionary genomics of archaea. *Biol Direct* **2**: 33.
- Makarova, K.S., Yutin, N., Bell, S.D., and Koonin, E.V. (2010) Evolution of diverse cell division and vesicle formation systems in Archaea. *Nat Rev Microbiol* **8**: 731–741.
- Margolin, W. (2009) Sculpting the bacterial cell. *Curr Biol* **19**: R812–R822.
- Nunoura, T., Oida, H., Nakaseama, M., Kosaka, A., Ohkubo, S.B., Kikuchi, T., *et al.* (2010) Archaeal diversity and distribution along thermal and geochemical gradients in hydrothermal sediments at the Yonaguni Knoll IV hydrothermal field in the Southern Okinawa trough. *Appl Environ Microbiol* **76**: 1198–1211.
- Pollard, T.D., and Cooper, J.A. (1986) Actin and actin-binding proteins. A critical evaluation of mechanisms and functions. *Annu Rev Biochem* **55**: 987–1035.
- Pollard, T.D., and Cooper, J.A. (2009) Actin, a central player in cell shape and movement. *Science* **326**: 1208–1212.
- Poole, A.M., and Penny, D. (2007) Evaluating hypotheses for the origin of eukaryotes. *Bioessays* **29**: 74–84.
- Roeben, A., Kofler, C., Nagy, I., Nickell, S., Hartl, F.U., and Bracher, A. (2006) Crystal structure of an archaeal actin homolog. *J Mol Biol* **358**: 145–156.
- Sonobe, S., Aoyama, K., Suzuki, C., Saito, K.-H., Nagata, K., Shimmen, T., and Nagata, Y. (2010) Proliferation of the hyperthermophilic archaeon *Pyrobaculum islandicum* by cell fission. *Extremophiles* **14**: 403–407.
- Stamatakis, A., and Ott, M. (2008) Efficient computation of the phylogenetic likelihood function on multi-gene alignments and multi-core architectures. *Philos Trans R Soc Lond B Biol Sci* **363**: 3977–3984.
- Trent, J.D., Kagawa, H.K., Yaoi, T., Olle, E., and Zaluzec, N.J. (1997) Chaperonin filaments: the archaeal cytoskeleton? *Proc Natl Acad Sci USA* **94**: 5383–5388.
- Vats, P., and Rothfield, L. (2007) Duplication and segregation of the actin (MreB) cytoskeleton during the prokaryotic cell cycle. *Proc Natl Acad Sci USA* **104**: 17795–17800.
- Woese, C.R., Kandler, O., and Wheelis, M.L. (1990) Towards a natural system of organisms: proposal for the domains Archaea, Bacteria, and Eucarya. *Proc Natl Acad Sci USA* **87**: 4576–4579.
- Yutin, N., Wolf, M.Y., Wolf, Y.I., and Koonin, E.V. (2009) The origins of phagocytosis and eukaryogenesis. *Biol Direct* **4**: 9.
- Zillig, W., Tu, J., and Holz, I. (1981) Thermoproteales – a third order of thermoacidophilic archaeobacteria. *Nature* **293**: 85–86.